CHAPTER I

Snell Midpoint Coordinates

1.1. Introduction.

Seismic data is usually collected in shot, geophone, depth and time coordinates. (s,g,z,t). Data processing and interpretation are done either in (s,g,z,t) coordinates or in midpoint, offset, depth, time (y,h,z,t) coordinates. Formulations of the double square root equation (Stolt, 1968; Claerbout, 1982) either in (s,g,z,t) or in (y,h,z,t) result in wavefield extrapolation operators that can image satisfactorily energy propagating close to the vertical. However, unless the exact medium velocity is known and the data follows the wave equation model perfectly, it is impossible to model wide propagation angles. For velocity estimation we need velocity independent wavefield extrapolators that could be used at wide propagation angles, there the data is more sensitive to velocity. None of the standard coordinate frames proves to be convenient.

In this chapter we introduce Snell midpoint coordinates. This frame of reference is specifically formulated to study slant wave propagation in the earth. The Linear Moveout (LMO) method of velocity estimation follows from the definition of Snell coordinates. With this method it is possible to estimate interval velocity using a fixed slant reference wavefront. Velocity estimation is accurate at all non-zero propagation angles. We analyze the properties of the LMO method and discuss the non-uniqueness of interval velocity estimates.

In chapter (IV) the double square-root equation will be formulated in Snell midpoint coordinates. In this coordinate system we can define wavefield extrapolators at wide propagation angles that are relatively insensitive to velocity.

Exploiting this property it will be possible to define the wave equation velocity spectrum.

1.2. Snell midpoint coordinates.

Studying wave propagation problems in the earth, it is customary to use plane vertically traveling reference wavefronts. An alternative approach is given by *slant* reference plane waves. These waves leave the surface at some non–zero takeoff angle. A slant wavefront has one of its components traveling laterally. This lateral component preserves information of the material properties the medium.

In stratified media Snell's parameter p, which is the horizontal component of the phase velocity, remains constant during propagation. A *Snell wave* is defined as a wave that has a fixed Snell's parameter p attached to it throughout its propagation. At the surface, since $p = \frac{\sin\vartheta}{v}$, to each departure angle there is a unique ray parameter p. As the wavefront travels, it will be refracted by changes in material properties with depth, but p will remain constant. Because of this property, Snell waves can be identified when they get reflected back to the surface.

From figure (2.1) we can see that when a slanted wavefront is leaving the surface at some offset h, the same wavefront has already traveled to depth z at the origin. Similarly, if the velocity of the medium is v the ray, perpendicular to the wavefront from the origin, has traveled a distance vt. Computing the travel-times to positions $(h, z=0)$ and $(h=0, z)$ give for the horizontal and vertical components of the phase velocity (v_H, v_V)

$$v_H = \frac{v}{\sin\vartheta} \geq v \tag{2.1}$$

$$v_V = \frac{v}{\cos\vartheta} \geq v \tag{2.2}$$

We also have that a reflected slanted wavefront from depth z will not arrive at zero offset, its arrival coordinates are

$$h = \int_0^z \tan\vartheta(\xi)\, d\xi \tag{2.3}$$

$$t = 2\int_0^z \frac{\cos\vartheta(\xi)}{v(\xi)} d\xi \tag{2.4}$$

From these equations we can see that the arrival offset at the surface depends

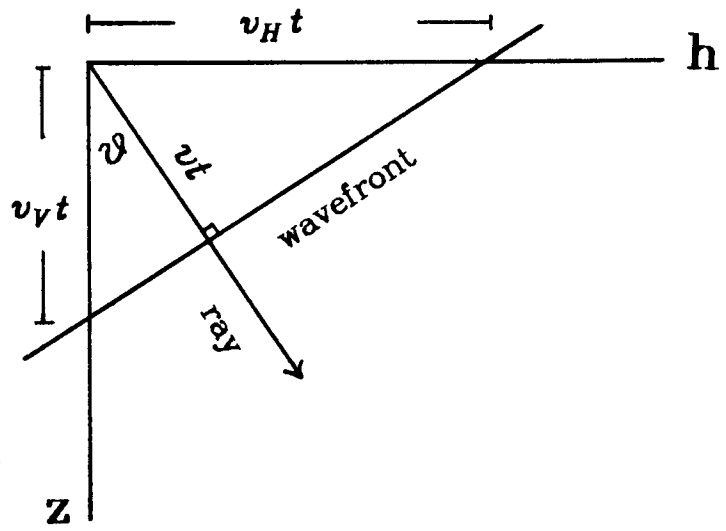

FIGURE 2.1. Slant wave propagation.

on the velocity structure of the medium. Velocity information is not lost. Our reference travel time is for the vertical component of the wavefront. This component travels with velocity v_V which is always greater or equal to the medium velocity. The minimum travel-time is less than the zero offset travel-time.

Snell midpoint coordinates are defined as

$$t' = t - p_0(g - s) + 2\int_0^z \frac{[1 - p_0^2 v^2(\xi)]^{1/2}}{v(\xi)} d\xi \tag{2.5a}$$

$$y = \frac{g + s}{2} \tag{2.5b}$$

$$h = \frac{g - s}{2} + \int_0^z \frac{p_0 v(\xi)}{[1 - p_0^2 v^2(\xi)]^{1/2}} d\xi \tag{2.5c}$$

$$\tau = 2\int_0^z \frac{[1 - p_0^2 v^2(\xi)]^{1/2}}{v(\xi)} d\xi \tag{2.5d}$$

These equations allow us to transform data from field coordinates into slant coordinates at any given depth. Figure (2.2) illustrates the geometric relationships. p_0 fixes the angle of the reference slanted Snell wave. In Snell Coordinates all arrivals with the reference ray parameter p_0 will have the minimum traveltime of a given event. In the next section we describe a method to estimate velocity using the arrival coordinates of a reference Snell wave.

1.3. Velocity estimation in Snell Midpoint Coordinates: LMO method.

Claerbout (1982) introduced a direct velocity estimation procedure using Snell waves. The method is a direct consequence of Snell midpoint coordinates at the image point. In this method velocity is determined as a function of arrivals associated with a slanted reference wavefront. In a stratified earth this treatment is exact for all non– zero offsets. The method requires the data in Snell

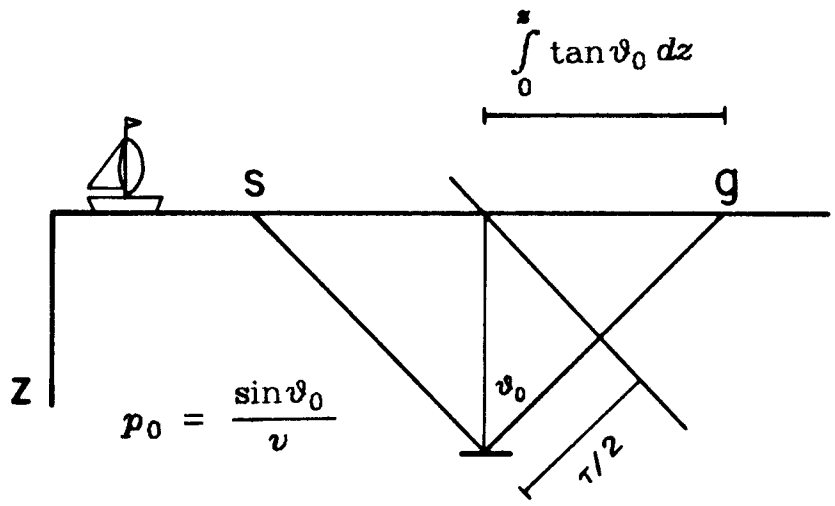

FIGURE 2.2. Snell Midpoint Coordinates.

midpoint coordinates. From equation (2.5) Snell midpoint coordinates at the surface of the earth ($z = 0$) are:

$$t' = t - p_0(g - s) \tag{3.1a}$$

$$y = \frac{g + s}{2} \tag{3.1b}$$

$$h = \frac{g - s}{2} \tag{3.1c}$$

$$\tau = 0 \tag{3.1d}$$

The data, therefore, needs to be sorted into midpoint–offset coordinates. Time should be modified with (equation 3.1a). This correction is commonly referred as *linear moveout correction (LMO)* to distinguish it from the Normal moveout *NMO* dynamic correction. This method of estimating velocity will be referred as the *LMO* method from now on.

From the last section we know Snell midpoint coordinates preserve velocity information. To find velocity, insert the imaging conditions $s = g$ and $t = 0$ in the definitions of Snell coordinates to get at fixed midpoint

$$t' = \tau \tag{3.2a}$$

$$h = \int_0^z \frac{p_0 v(\xi)}{[1-p_0^2 v(\xi)^2]^{1/2}} d\xi \tag{3.2b}$$

$$\tau = 2\int_0^z \frac{[1-p_0^2 v(\xi)^2]^{1/2}}{v(\xi)} d\xi \tag{3.2c}$$

With $\frac{dh}{dz}$ and $\frac{d\tau}{dz}$ we can use the chain rule to eliminate dz and solve for velocity:

$$v^2 = \frac{1}{p_0\left[p_0 + \frac{1}{2}\frac{d\tau}{dh}\right]} \tag{3.3}$$

When the reference ray parameter is zero, this equation is indeterminate, implying velocity information is not available at zero offset. Equation (3.3) is valid at any depth of observation.

Using equation (3.3) we can estimate velocity directly from the data. The ray parameter p_0 fixes the departure angle of the reference wavefront. The slope $\frac{d\tau}{dh}$ is measurable directly from the data. We consider two alternatives to measure this slope. It can be measured from the origin, or it can be measured between two consecutive primary arrivals. What velocity is being measured?.

First notice that the slanted time τ_0 is not equal to the vertical time t_0; a cosine correction needs to be done. Assuming velocity can be parameterized in different variables

$$v(z) = v_\tau(\tau(z)) = v_t(t(z))$$
$$\vartheta(z) = \vartheta_\tau(\tau(z)) = \vartheta_t(t(z))$$

The observed τ_0 in slanted coordinates is given by

$$\tau_0 = 2\int_0^z \frac{[1 - p_0^2 v^2(\xi)]^{1/2}}{v(\xi)} d\xi \tag{3.4}$$

while the vertical traveltime is

$$t_0 = 2\int_0^z \frac{1}{v(\xi)} d\xi \tag{3.5}$$

Combining equations (3.4) and (3.5) yields

$$\tau_0 = \int_0^{t_0} [1 - p_0^2 v_t^2(\xi)]^{1/2} d\xi \tag{3.6}$$

$$t_0 = \int_0^{\tau_0} \frac{1}{[1 - p_0^2 v_\tau^2(\xi)]^{1/2}} d\xi \tag{3.7}$$

or, approximating the propagation angle to a constant $\cos\bar{\vartheta}_0 = [1 - p_0^2 \bar{v}^2]^{1/2}$,

$$t_0 = \frac{\tau_0}{\cos\bar{\vartheta}_0} \tag{3.8}$$

If t_0 is not picked directly from the data, this equation shows how to find it from the image positions τ_0. The depth is given by

$$z = \frac{1}{2}\int_0^{\tau_0} \frac{v_\tau(\xi)}{[1 - p_0^2 v_\tau^2(\xi)]^{1/2}} d\xi = \frac{1}{2}\int_0^{t_0} v_t(\xi)\, d\xi \tag{3.9}$$

To find what velocity the LMO method measures, by combining equations (3.2) and (3.6) we can write the arrival offset h as a function of τ

$$h = \frac{1}{2}\int_0^{\tau} \frac{p_0 v_\tau(\xi)^2}{1 - p_0^2 v_\tau(\xi)^2} d\xi$$

or since $\cos^2\vartheta_\tau = 1 - p_0^2 v_\tau^2$

$$h = \frac{1}{2} p_0 \int_0^{\tau} \frac{v_\tau(\xi)^2}{\cos^2\vartheta_\tau(\xi)} d\xi \tag{3.10}$$

We can think of replacing the velocity structure in stratified media by a single layer with constant velocity $\bar{v}$. This statistically represents the velocity structure of the rock column. Replacing $\bar{v}$ in equation (3.10) gives*

$$h = \frac{1}{2} \frac{p_0 \bar{v}^2 \tau}{\cos^2\bar{\vartheta}} \tag{3.11}$$

Solving for $\bar{v}^2$

$$\bar{v}^2 = 2 \frac{\cos^2\bar{\vartheta}}{p_0} \frac{h}{\tau} \tag{3.12}$$

replacing h by the expression of equation (3.10) yields

$$\frac{\bar{v}^2}{\cos^2\bar{\vartheta}} = \frac{1}{\tau}\int_0^{\tau} \frac{v_\tau(\xi)^2}{\cos^2\vartheta_\tau(\xi)} d\xi \tag{3.13}$$

We can rewrite this equation as function of the two-way traveltime t

$$t = \int_0^{\tau} \frac{1}{\cos^2\vartheta_t(\xi)} d\xi \equiv \frac{\tau}{\cos^2\bar{\vartheta}} \tag{3.14}$$

to obtain

---

*Since h and τ are fixed, errors in this approximation will affect the depth z.

$$\bar{v}^2 = \frac{1}{t}\int_0^t v_t(\xi, p_0)^2 \, d\xi \equiv v_{RMS}^2(p_0) \tag{3.15}$$

This is Dix's equation. Constant velocity $\bar{v}$ in equations (3.2b) and (3.2c) give the relation

$$\bar{v}^2 = \frac{1}{p_0\left(p_0 + \frac{1}{2}\frac{\tau}{h}\right)} \tag{3.16}$$

Therefore, the slope τ/h from the origin gives an estimate of the RMS velocity. (Figure 3.1). This v_{RMS} is not unique, it depends on angle.

Instead, if we measure the slope between two consecutive primary events, from equation (3.2) we have

$$\Delta h = h_{i+1} - h_i = \frac{1}{2}p_0\int_{\tau_i}^{\tau_{i+1}} \frac{v_\tau(\xi)^2}{\cos^2\vartheta_\tau(\xi)}\, d\xi \tag{3.17}$$

Assuming constant *interval* velocity between the events and solving for velocity, we get

$$v_{interval}^2 = \frac{1}{p_0\left(p_0 + \frac{1}{2}\frac{\Delta\tau}{\Delta h}\right)} \tag{3.18}$$

Therefore, when velocity remains constant between any two consecutive primary arrivals, equation (3.3) gives their interval velocity. (Figure 3.1). When velocity varies appreciably between reflectors, interval velocity is unresolved with reflection traveltime data alone. Equation (3.3) gives then a local RMS velocity estimate for the particular choice of p_0. In the next section we analyze this situation.

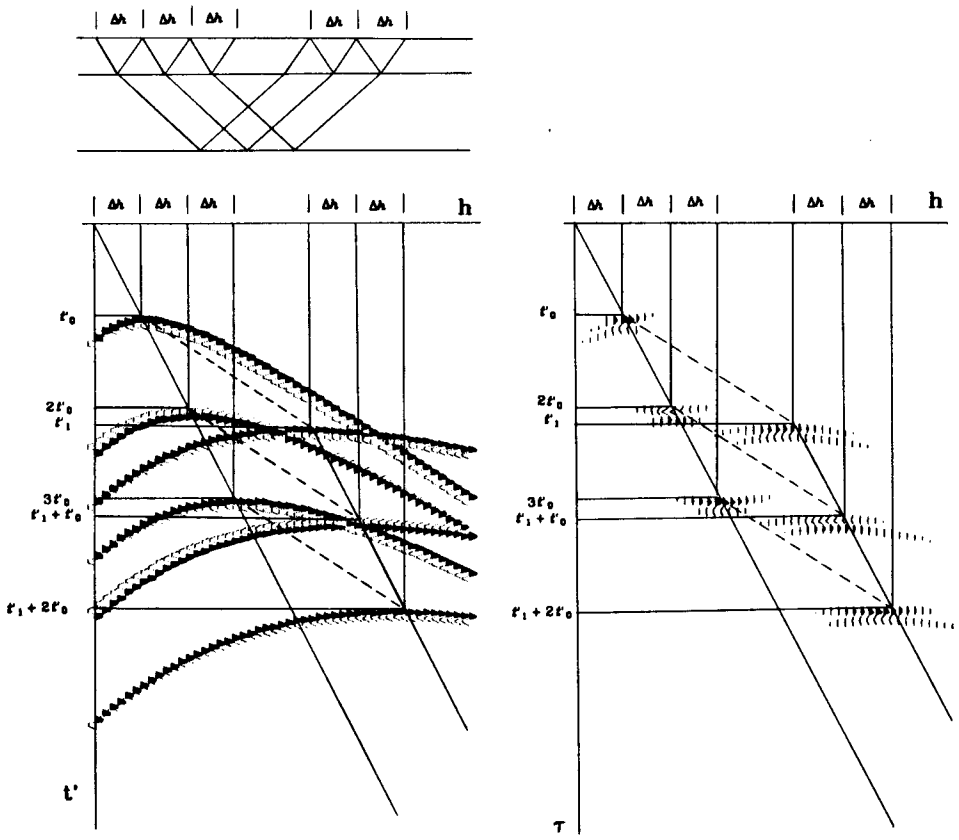

FIGURE 3.1. Linear velocity estimation. (a) Synthetic *CMP* with LMO applied. The data shows arrivals for two primary reflectors, two multiples and two peg–leg multiples. The reference Snell wave for the first primary has arrival coordinates $(\Delta h, t'_0)$; the first multiple $(2\,\Delta h, 2\,t'_0)$; and the second multiple $(3\,\Delta h, 3\,t'_0)$. Similarly the reference Snell wave for the second primary arrives at location (h_1, t'_1); the first peg–leg multiple at $(h_1 + \Delta h, t'_1 + t'_0)$; and the second peg–leg multiple at $(h_1 + 2\,\Delta h, t'_1 + 2\,t'_0)$. The interval velocity for the second medium is a function of the slope between the reference Snell wave arrivals for the first and the second primaries, that is, the slope of the first dashed line. Snell midpoint coordinates preserve the timing and offset relationships of multiple reflections, thus the interval velocity can also be estimated measuring the slope between the reference Snell wave arrivals for the i^{th} multiple and peg–leg multiple. Raypaths for the reference Snell wave arrivals are shown at the top. (b) Wave equation image of the data. In Snell midpoint coordinates velocity estimation can be done at any depth of observation, therefore with the image of the data itself. (Chapter IV).

It is emphasized that in obtaining equations (3.3) and (3.18) no geometrical approximations were made. The horizontal coordinate of the wavefront has velocity information and these relationships show how to find it. A convenient

way of measuring velocity is to tabulate equation (3.3) for a fixed value of the ray parameter p_0. This is shown in figure (3.2).

As pointed out by Schultz (1981), more accurate interval velocity estimates should be used as an interpretation tool more than as a processing tool. Accurate interval velocities do not necessarily imply better stacking velocities. They do imply better migration velocities.

When there is a geologic dip component with angle α, Levin (1971) proved that v_{NMO} obtained using Taner and Koehler's method is v_{RMS} modified by the cosine of the dip angle

$$v_{NMO} = \frac{v_{RMS}}{\cos \alpha} \tag{3.19}$$

This result is valid when slanted reference waves are used.

More realistically, the data may have events with several dips. Pre–stack partial migration can be applied prior to velocity estimation to obtain a more accurate dip compensation. (Sherwood *et al*, 1976; Yilmaz and Claerbout, 1980; Deregowski and Rocca, 1981; Ottolini, 1982; Hale, 1982).

The LMO method has important advantages. This method can be used in the far offsets where data has more velocity resolution. The method is flexible in that we can select a value of p_0 where the signal–to–noise ratio of the data is particularly good. Transformation to Snell midpoint coordinates is linear. Also there is more control in deciding what events to use in the velocity estimation process. Multiple reflections preserve their timing relationships, becoming easier to discriminate against primaries. This method is also partially insensitive to refractions and cable truncations.

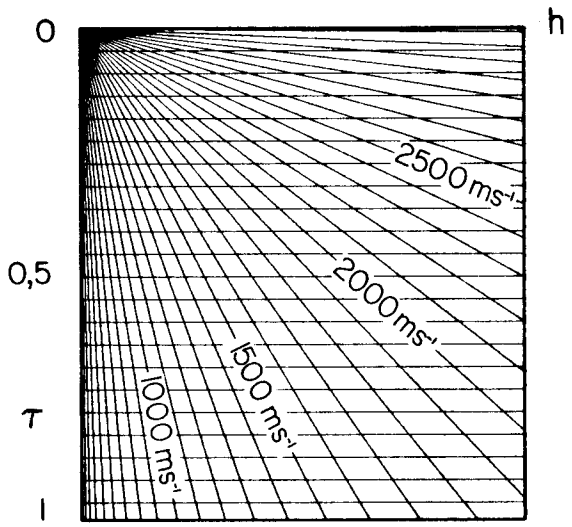

FIGURE 3.2. Velocity estimation grid. This grid is a tabulation of equation (3.3) for a fixed value of Snell's parameter p_0. The slope from the origin gives the *RMS velocity*, the slope between two consecutive primary events gives their *Interval velocity*.

1.4. Non-uniqueness of velocity estimates.

In the last section we proved that in stratified earth with flat reflectors and no velocity variations between reflectors, the LMO method could be used to get consistent interval velocity estimates at any propagation angle. The LMO method can also estimate RMS velocities according to Dix's equation.

When there are velocity variations between reflectors, reflection data alone cannot give unique velocity estimates. The problem is underdetermined. This may happen either when there are continuous velocity inhomogeneities between reflectors (infinite unknowns), or if the interval velocity is measured between non–consecutive primary arrivals.

The LMO method is sensitive to velocity variations between reflectors. We can use Snell midpoint coordinates to find criteria to decide when these velocity inhomogeneities are not negligible. If this is the case, velocity estimation

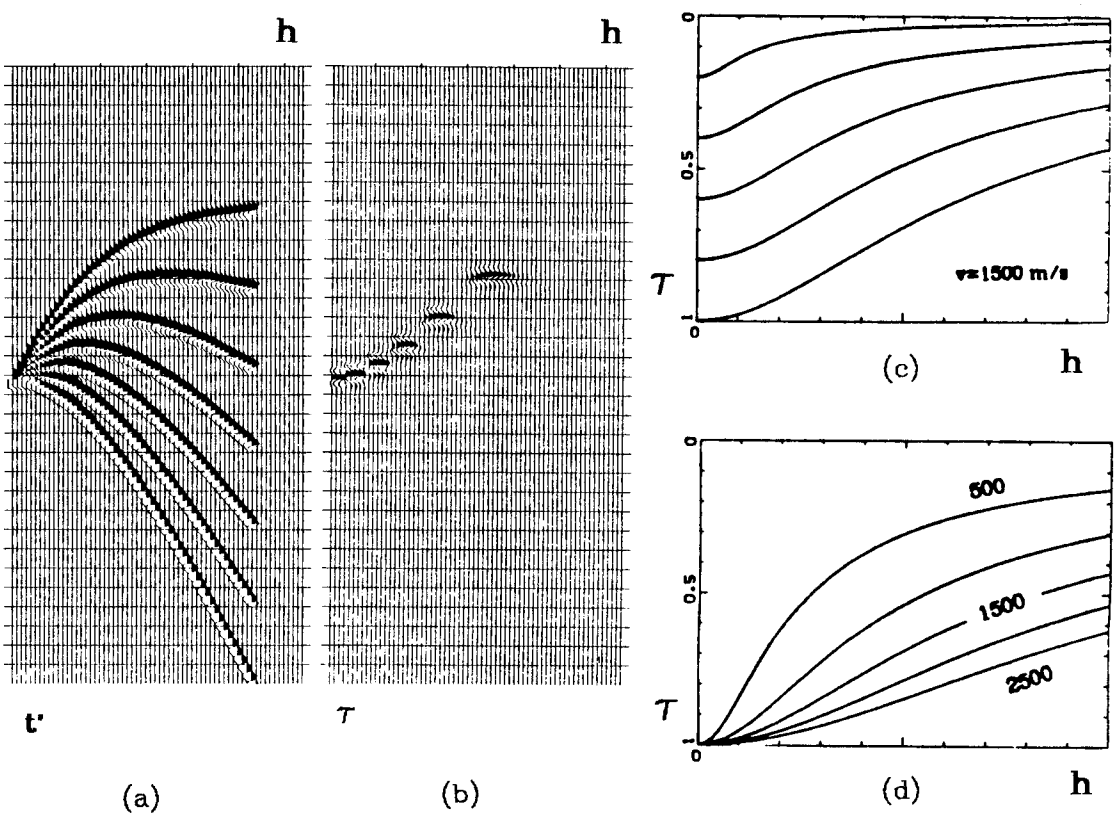

FIGURE 4.1. Image coordinates as function of p_0. (a) Superposition of synthetic CMP gathers. A LMO correction has been applied with different p_0 before superposition for display. Reference event has $v = 1500\ m/sec$. (b) Imaged CMP gathers. In this diagram it is easy to follow the trajectory of the reference Snell wave arrivals for different p_0. (c) $\tau_0\ vs\ h$ diagram. This trajectory will be followed by reference Snell wavefronts arrivals with increasing ray parameter p_0. Velocity is constant, different time-depths. (d) Same as (c) with variable velocity and fixed time-depth. The range of offsets is 1575 m, time is in seconds.

methods with refraction data, such as the wavefield continuation method of Clayton and McMechan (1981) or the tau-sum inversion method of Diebold and Stoffa (1981), should give better velocity estimates. Refraction methods, however, do not detect velocity reversals.

Reconsidering the question of what velocity the LMO method measures; from equations (3.17) and (3.18) we know that if the velocity remains constant between any two reflectors, then the interval velocity estimate is independent of

the reference p_0. If we measure interval velocity at any two locations p_1 and p_2, then

$$1 = \frac{p_1 \left(p_1 + \frac{1}{2} \frac{\Delta\tau}{\Delta h} \middle| p_1 \right)}{p_2 \left(p_2 + \frac{1}{2} \frac{\Delta\tau}{\Delta h} \middle| p_2 \right)} \tag{4.1}$$

As velocity inhomogeneities between reflectors increase, the concept of interval velocity becomes meaningless. To see this, from equation (3.13) we have

$$\frac{\bar{v}^2}{\cos^2\bar{\vartheta}} = \frac{1}{\tau_{i+1}(p_0) - \tau_i(p_0)} \int_{\tau_i(p_0)}^{\tau_{i+1}(p_0)} \frac{v_\tau(\xi)^2}{\cos^2\vartheta_\tau(\xi)} d\xi \tag{4.2}$$

i.e. interval velocity measurements become local angle–dependent RMS velocity estimates.

With equation (4.2) we can quantify whether velocity variations are negligible or not. Defining an error function $\varepsilon(p_1, p_2)$ as

$$\varepsilon(p_1, p_2) \equiv 1 - \frac{p_1 \left(p_1 + \frac{1}{2} \frac{\Delta\tau}{\Delta h} \middle| p_1 \right)}{p_2 \left(p_2 + \frac{1}{2} \frac{\Delta\tau}{\Delta h} \middle| p_2 \right)} \tag{4.3}$$

With ε we can quantify when the interval velocity estimates show angle variations above the measurement uncertainties. That could show there are strong velocity variations between reflectors. A convenient way to test this is to plot the expected *vs* the observed image locations as function of p_0 in the (h, τ) plane. (Figure 4.1)